Check for updates

Advances in Mechanical Measurement and Control of Composite Structures - Research Article

Advances in Mechanical Engineering

Advances in Mechanical Engineering
2021, Vol. 13(4) 1–13
© The Author(s) 2021
DOI: 10.1177/16878140211995703
journals.sagepub.com/home/ade
SAGE

Optimisation for clamping force of aircraft composite structure assembly considering form defects and part deformations

Wei Zhang[1,2], Luling An[1], Yuan Chen[3], Yeping Xiong[4] and Yabing Liao[3]

Abstract

Given the existence of manufacturing defects and the accumulation of assembly errors, non-compliant assembly appears between components, especially for composite structure assembly. In the engineering application, the clamping force (CF) is often used to eliminate the clearance between mating components, but the improper CF may result in unwanted structure failure. Thus, on the premise of ensuring the safety of composite parts, this study proposes a procedure to systematically optimise the assembly CF. Firstly, the components mating surfaces were obtained by laser scanner, and the matching of actual surfaces was transformed and simplified based on 'equivalent surface' concept. Then, a mathematical optimisation model was established. The CF layout and magnitude were taken as variables, and the clearance elimination rate and the overall assembly force value were employed as objective functions. Finally, the improved genetic algorithm (GA) was used to solve this problem. A parametric finite element analysis (FEA) model was built, and model accuracy was verified by physical experiments. The finite element calculation and post-processing were carried out by Python script in ABAQUS®. Compared to the engineer's traditional approach, the influence of form defects and part deformations were considered, which can help control the assembly stress well and ensure product performance.

Keywords

Composite damage, aircraft assembly, form defects, part deformations, genetic algorithm

Date received: 21 September 2020; accepted: 8 January 2021

Handling Editor: James Baldwin

Introduction

In the aircraft-manufacturing industry, composite materials bring improved design, performance and weight-saving characteristics due to its excellent mechanical properties. Whether it is the increasement of composite material usage or the expansion of application range, composite materials changed the traditional aircraft structure design and manufacturing significantly. However, given the deviation in the manufacturing process, the forming precision of the composite component is not high, coupled with the spring forward impact after manufacturing, the composite

[1]College of Mechanical and Electrical Engineering, Nanjing University of Aeronautics and Astronautics, Nanjing, China
[2]School of Aerospace, Transport and Manufacturing, Cranfield University, Bedford, UK
[3]College of Engineering, Nanjing Agricultural University, Nanjing, China
[4]Engineering and Physical Sciences, University of Southampton, Southampton, UK

Corresponding author:
Luling An, College of Mechanical and Electrical Engineering, Nanjing University of Aeronautics and Astronautics, Nanjing 210016, China.
Email: anllme@nuaa.edu.cn

Creative Commons CC BY: This article is distributed under the terms of the Creative Commons Attribution 4.0 License (https://creativecommons.org/licenses/by/4.0/) which permits any use, reproduction and distribution of the work without further permission provided the original work is attributed as specified on the SAGE and Open Access pages (https://us.sagepub.com/en-us/nam/open-access-at-sage).

component inevitably produces geometric deviations, which makes the actual shape of the component deviate from the theoretical one. Moreover, composite laminate is an anisotropic material, and the mechanical properties in thickness-direction are significantly weaker than the performance of the fibre plane. Resultantly, assembly stress causes local damage easily, which will continuously grow with the local deformation during its service and will lead to premature failure, which greatly reduces the component life and reliability. Therefore, in composite structure assembly, high requirements for assembly coordination and stress control are put forward, and it is equally important to control the assembly stress level and ensure the assembly accuracy.

The wing is one of the important parts of an aircraft, and the wing box structure is composed of an upper panel, a skeleton (contains ribs and spars) and a lower panel. There is a strict relationship between the components to ensure assembly structure accuracy. However, geometric deviations are inevitably occurred in product manufacturing,[1,2] leading to assembly gap between the mating components. Given that the components cannot fit tightly with one another, the gaps could lead to a non-compliant assembly and increase the assembly stress. In the literature, numerous research topics were conducted to reduce the assembly stress of composite structures. Ramirez and Wollnack[3] proposed a flexible automatic assembly method for large composite structure, which can adjust component posture by a flexible unit to actively control the tolerance allocation. This best-fit assembly posture can reduce shim usage. A separate paper of our previous research work[4] adopted the method of measurement assisted assembly to optimise and adjust the position and posture of the wing box panel according to the actual gap values to realise the active distribution of the assembly gap. Zhang et al.[5] proposed an optimisation method to optimise the pressing force of the assembly gap in composite airframe structure, but the gap is idealised as a uniform gap, which cannot reflect the actual situation. Moreover, the magnitude of the pressing force was not optimised separately. In view of the mixed assembly of metal/composite components, Maropoulos et al.[6] proposed a method to obtain the actual size of composite structure through high-precision scanning measurement in the assembly process, which can precisely process or fettle the metal material components to realise the coordination and installation of components and finally avoid the assembly stress generated by the interference problem. Jonsson[7,8] studied a flexible part positioning method on the basis of force control to complete the assembly by constantly monitoring the assembly force and torque. Wu et al.[9] determined the degree of panel compaction on the basis of direct force control strategy and optimised the size of the compression force on the panel to eliminate the assembly gap. Söderberg et al.[10] applied the influence coefficient method to establish the numerical response model between the parts manufacturing deviation, the fixture positioning deviation and the assembly stress of the composite wing rib and analysed the statistical distribution of the assembly stress in the wing rib.

Most of the above studies on assembly technology of composite structure focus on reducing or controlling the distribution of assembly gap before the applied assembly force to prevent excessive assembly stress caused by overlarge gap. However, no monitoring and evaluation were carried out during the assembly force application. Some research works directly measured and controlled the assembly force to improve the internal stress distribution or eliminate assembly clearance but did not simultaneously consider the influence of assembly stress and assembly clearance. Also, literatures on the assembly force limitation[11] applied to the composite structure and the effect of force distribution on the whole structure were rarely published.

Assembly tooling is used to locate, clamp and connect the assembly components. For thin-walled structures, 'N-2-1' locating principle is widely used to accurately locate the component. The priority of this positioning method is adopting different fixture layouts to reduce part deformation caused by support fixtures. Regarding the fixture locating layout optimisation, scholars conducted substantial research on this field. Krishnakumar and Melkote[12] used GA to find the fixture layout that minimised the deformation of the machined surface. Padmanaban et al.[13] presented an ant colony algorithm (ACA) on the basis of discrete and continuous optimisation methods to search the optimal machining fixture layout so that the workpiece elastic deformation was minimised. Cheng et al.[14] proposed a hierarchical fixture layout model to decrease the assembly variation of aeronautical thin-walled structure. The base points and locating points were optimised by GA and ACA. Lu and Zhao[15] combined the GA and back propagation neural network model to optimise the fixture layout for the sheet metal workpiece on the basis of the 4-2-1 locating scheme. Yang et al.[16] presented a combined cuckoo search algorithm with FEA to optimise the sheet metal fixture locating layout. Chen et al.[17] proposed a kind of flexible fixture for car dashboards based on a new N-M principle. Most of the above literatures simply studied the impact of support fixture layout on part deformation but did not cover the impact on the assembly stress of the entire structure. Moreover, most of the studies focused on the locating of thin-walled metal parts, which is not fully applicable to composite structure assembly.

Given that composite is anisotropic material, it has complicated failure modes and diverse damage types. For composite laminates, the basic damage modes

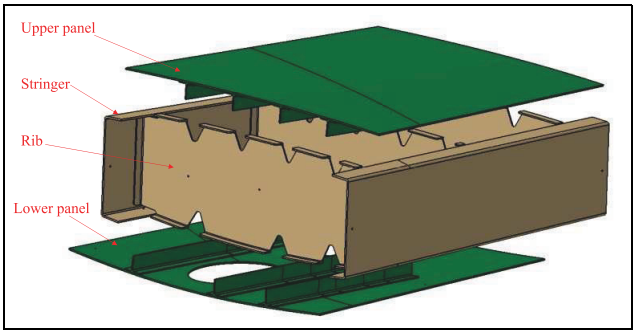

Figure 1. Wing box structure.

include intralaminar damage (matrix cracking), interlaminar damage (interior delamination) and fibre rupture. To avoid failure of composite laminates, the complicated mechanism between normal (σ_{11}, σ_{22}, σ_{33}) and shear stresses (τ_{23}, τ_{31}, τ_{12}) should be considered comprehensively to determine the assembly force. Therefore, in this study a new multivariable optimisation method by integrating improved GA and FEA is proposed for the assembly force design of composite structures. The cohesive zone model is inserted into the parametric FEA model to predict the composite damage. The layout and magnitude of the CF scheme are optimised to effectively improve the distribution of assembly gap between components and avoid the damage of composite structure caused by stress concentration simultaneously. The remainder of this paper is organised as follows: Section 2 illustrates the assembly procedure of composite wing box panel and the mathematical model for the assembly CF optimisation. On the basis of the 'equivalent surface' method, the form defects of the components are considered into the optimisation model, and the constraint criteria for internal damage of composite structure is analysed emphatically. Section 3 presents the construction flowchart for the CF layout and magnitude optimisation on the basis of improved GA. A case study is conducted in Section 4 to demonstrate the implementation procedures, which includes the FEA model verification by comparing the simulated results with the experimental data and the efficiency validation of the optimisation algorithm. Finally, Section 5 summarises.

Optimisation problem formulation

Assembly procedure of composite wing box panel

Figure 1 illustrates the aircraft wing box structure. The wing box comprises the upper panel, the skeleton (including the stringers and ribs) and the lower panel. Here, we focus on the assembly of upper panel and skeleton. As illustrated in Figure 2, the upper panel is positioned by assembly tooling based on the 'N-2-1'

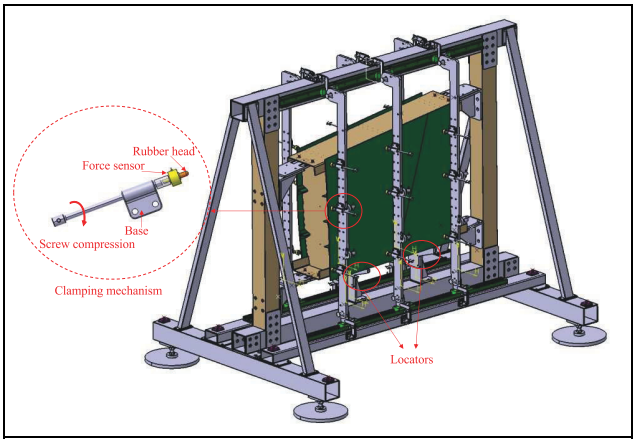

Figure 2. Wing box upper panel assembly.

locating principle. The bottom and side of the panel as the secondary and tertiary datum are respectively positioned by the locators. On the primary datum, the CF is provided by a clamping mechanism and applied to the panel. The clamping mechanism adopts screw compression, and the head is equipped with force sensors, which can monitor and adjust the CF in real time. The CF is used to eliminate the assembly gap between the mating surfaces as much as possible, so that the panel and the skeleton can better fit together. However, due to the scattered distribution and large spatial span of the assembly gap, it cannot be eliminated by a single point of CF. Therefore, it is necessary to optimise the arrangement of the CF scheme to eliminate more gaps and complete high-quality assembly. In this study, our interests focus on the optimisation of CF layout and magnitude in the wing box structure assembly to minimise the overall gap between the mating components (the panel and the skeleton) and optimise the assembly stress distribution within the structure. Thus, the assembly CF optimisation is regarded as a highly nonlinear optimisation problem with multiple variables and constraints.

Laser-scanning measurement technology is widely used in aircraft assembly and helps measure the key features precisely. By scanning the key mating surfaces between the panel and the skeleton, 3D surface data can be obtained. Therefore, evaluating the gaps of the whole faying surfaces efficiently and precisely is possible. For the purpose of adjusting the assembly CF on the basis of the actual assembly situation, the inner surface of the panel and the corresponding mating surface of the skeleton are obtained by optical measurement system. Then, the assembly procedure in which the panel tries to fit into the skeleton under the CF can be expressed as two non-ideal surfaces that are fitted together by applying external forces, as illustrated in Figure 3.

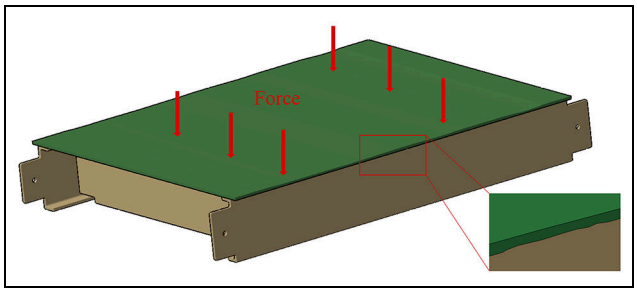

Figure 3. Mating surface of two non-ideal components.

To simplify this numerical assembly phase, the artifact of 'equivalent surface' concept is applied.[18,19] The core ideas of this concept are expressed as follows: under the assumption of non-adhesive contact, the contact between two non-ideal surfaces can be replaced by the contact between an ideal flat surface and an equivalent non-ideal surface.[20–22] The obtained distributions of the contact gap distance for these two situations are identical. This replacement process is illustrated in Figure 4, where Surfaces 1 (Ω_1) and Surfaces 2 (Ω_2) represent two non-ideal surfaces in contact. Ω is the equivalent non-ideal surface, and it can be obtained by $\Omega = \Omega_1 - \Omega_2$. In this study, $\Omega_1 = \{p_i\}_{i=1}^{M}$ and $\Omega_2 = \{q_i\}_{i=1}^{N}$ are two discrete point cloud models obtained from laser scanner, where M and N are the number of points on surfaces Ω_1 and Ω_2, respectively. Here the nearest neighbour is used to establish the relationship between the two-point clouds, that is, for each point (q_i) on Ω_2, the corresponding point (p_{q_i}) on Ω_1 is determined on the basis of Euclidean distance $\boldsymbol{d}$, for example, $\boldsymbol{d}(\boldsymbol{k}(q_i), p_{q_i}) = \|\boldsymbol{k}(q_i) - p_{q_i}\|$. Let $q_i = (x_i, y_i, z_i)$, $q_i \in \Omega_2$, then the coordinates of the sampling points on the equivalent surface (Ω) can be expressed as $h_i = (x_i, y_i, d_i), h_i \in \Omega$. Therefore, on the basis of the 'equivalent surface' concept, the mating surfaces between the actual panel and skeleton can be converted to the matching between the ideal panel surface and the equivalent skeleton surface. The objective is to minimise the gap distribution between the two mating surfaces by adopting an ideal layout and small force value.

Optimisation model establishment

In the CF optimisation problem for composite wing box panel assembly, the key point of the algorithm is to optimise the layout and magnitude of the CF scheme so that the gap between the panel and the skeleton can be minimised and the constraint of no damage to composite panel can be satisfied simultaneously. In this problem, design variables include clamping points' positions and magnitudes. Two objectives (the maximum gap elimination rate and the minimum overall CF value) should be synchronously satisfied to obtain an optimal solution. The variables of this optimisation problem are discrete and discontinuous in the solution space. Also, the numerical relationship between the objectives and the variables cannot be expressed by the analytical formula. Thus, the FEA method is applied to model the composite wing box panel assembly and to calculate the objective values. Here, ABAQUS® is used to solve this optimisation problem, and Python script is adopted to conduct finite element calculation and post-processing, which can realise the automation of the whole iterative optimisation. The FEA model pre-processing, submission, calculation and post-processing can be fully programmed using Python scripts or secondary development. As the official scripting language of ABAQUS®, Python language has many advantages, such as expandability, portability, object oriented and embeddability. Hence, a parametric FEA model is established and the automatic optimisation of CF

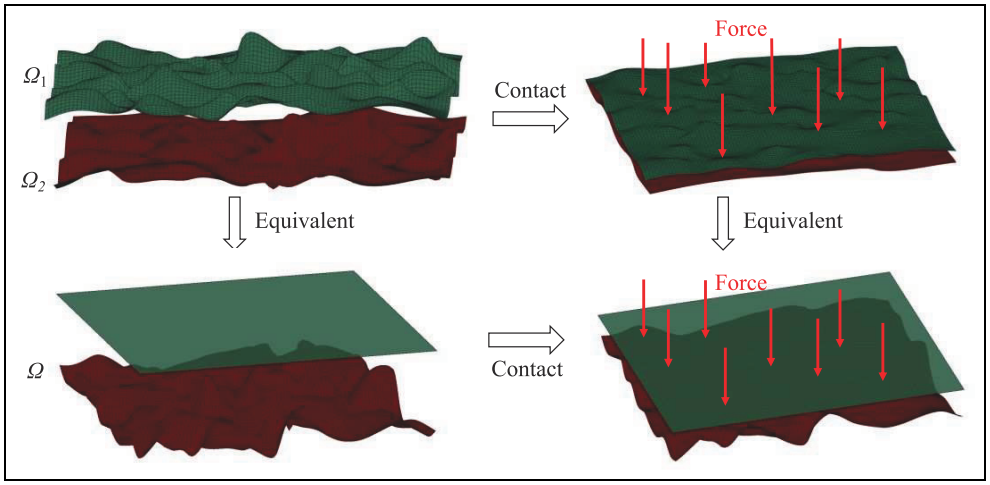

Figure 4. Replacement process of equivalent surface.

scheme is realised by Python scripts. Ultimately, the CF optimisation problem can be formulated as

$$\begin{aligned} &Find: X = \left[X_1 X_2 \cdots X_i \cdots X_j \cdots X_n\right], \\ &X_i = (d_i, F_i),\ \ d_i = (x_i, y_i) \end{aligned} \tag{1}$$

$$\begin{aligned} &Maximize: f^1(X) = \frac{1}{M}\sum_{i=1}^{M} h_i(X), \\ &h_i(X) = \begin{cases} 1, & if\, \omega_i(X) \leqslant \Delta\omega \\ 0, & if\, \omega_i(X) > \Delta\omega \end{cases}, \end{aligned} \tag{2}$$

$$\text{Minimize}: f^2(X) = \frac{\delta \times \sum_{i=1}^{n} F_i}{n \times F_{limit}}, \tag{3}$$

$$\begin{aligned} &\text{Subject to}: d_i \neq d_j,\ \ \left|d_i d_j\right| > L, \\ &d_i, d_j \in \Omega, 0 \leqslant F_i \leqslant F_{limit},\ \ K_s(X) < 1, \end{aligned} \tag{4}$$

where X represents the design variables, including the layout and the magnitude of the CF schemes; d_i and F_i denote the coordinate and the force value of the ith CF, respectively; L is the minimum safe distance allowed between two clamping points; n is the total number of the CF applied on the part; $f^1(X)$ depicts the gap elimination rate; M is the total number of the monitoring points; ω_i represents the gap value at this point; $\Delta\omega$ is a constant value; $f^2(X)$ depicts the overall assembly CF value; δ is worked as a weighting factor; F_{limit} is the threshold value that the structure can bear. In addition, all CF points must be in the predetermined domain Ω, and the clamping points in the same layout scheme cannot be overlapped. For $K_s(X) < 1$ means no damage occurred inside the composite structure.

The constraint criteria for internal damage of composite structure is one of the main concerns in this optimisation algorithm. Given that composite materials are anisotropic and heterogeneous, the applied CF can cause damage failure easily, especially when the assembly gap is large. Thus, setting the assembly force limit to ensure that the assembly stress induced by CF will not lead to internal damage of composite structure is necessary. Interior delamination is the most common damage type, which covers the majority in all the failure modes.[23] Therefore, in this study, the delamination damage is worked as a criterion for judging the feasibility of the CF scheme. Given the variety and complexity of composite structures, traditional fracture mechanics theory can no longer meet the research requirements of composite interface cracking. Moreover, a Cohesive Zone Model (CZM) based on elastoplastic fracture mechanics is increasingly used to calculate the interfacial damage of composites.[24,25] Thus, here, the delamination damage is predicted by inserting CZM into the parametric FEA model in ABAQUS®. Through the continuous attenuation of stiffness of cohesive element, the initiation and propagation of interlaminar cracks without initial defects are simulated to judge the delamination of composite materials.[26,27]

After the CZM is established, the QUADSCRT and SDEG values of the units can be queried to judge the delamination damage when forces are applied to the FEA model. QUADSCRT and SDEG represent the stress and damage state of the unit, respectively. The QUADSCRT value increases from 0 to 1 when the stress of the cohesion unit gradually increases from zero to the maximum. QUADSCRT equals to 1 means the stress reaches its maximum. Thereafter, as the load continues to increase, the stress will gradually decrease to zero and the SDEG value will increase from 0 to 1. When the maximum SDEG value reaches 1, it means that the cohesive unit is completely destroyed, and its loading capacity is lost. Thus, in this study the maximum SDEG value is used as a criterion for judging composite damage, represented by $K_s(X)$. $K_s(X) = 1$ indicates that the stiffness of some elements in the model has been completely degraded, and the structure has a delamination damage.

Multivariable optimisation based on improved genetic algorithm

Genetic algorithm (GA) is a computational model that mainly simulates the biological evolution process of natural selection and genetic mechanism in Darwin's biological evolution and genetic theory of Mendel and Morgan. It searches for the optimal solution by simulating the natural evolution process.[28] GA was first developed by Professor J. H. Holland in the University of Michigan in 1975.[29] The algorithm has been widely used in many fields, such as function optimisation, machine learning, image recognition and so on.[30] It can provide efficient solutions to some nonlinear, discrete variable, multi-design variable and multi-constraint optimisation problems.[31] Moreover, GA has few requirements on the relationship between design variables and objective functions. Also, the gradient information of the objective function is not needed yet. Therefore, GA is a good option to solve this multi-constraint optimisation problem. The complete procedure of CF optimisation for composite structure assembly comprises two main phases. Firstly, the optimisation model considering the actual form defects of mating components is established, which is regarded as the pre-processing of the optimisation algorithm. Then, on the basis of the FEA model, GA is conducted for optimisation calculation. The main steps of iterative calculation in ABAQUS® are described as follows:

Step 1. The parametric FEA model establishment, including the material properties definition, the ply

design of the component and damage judgement of the composite.

Step 2. The optimisation parameters setting, including the number of load point n, the safe distance allowed between two clamping points L, the feasible region Ω and the predetermined gap value $\Delta\omega$ and so on.

Step 3. Coding and variable initialisation. Coding is the basis of computing fitness function and genetic operator operation. In this study, binary coding is used to encode design variables. The initial generation group is generated randomly, and each group contains several individuals. One individual can represent a CF scheme. Here, assume that the assembly tooling can provide n CF points. X represents the population. $X = [X_1, X_2, \cdots, X_i, \cdots, X_j, \cdots, X_n]$, $X_i = (x_i, y_i, F_i)$. x, y coordinates and the force size for every clamping point can be expressed by one gene, respectively. Then every individual obtains $3n$ genes.

Step 4. Interference check and repair. In mathematical models, constraint processing technology is the key to solve the constraint optimisation problem, and common processing methods include penalty function, transformation and repair methods.[32,33] The repair method is converting the infeasible solution to the feasible one to avoid the invalid operation. In this algorithm, all individuals will be checked to judge the space distance between adjacent clamping points. If the distance is less than the safe distance L, then the latter clamping point will be removed and replaced by a new one.

Step 5. Finite element analysis, including the model reset, submission of input file, finite element calculation and the output of the result file. First, modify the ABAQUS® simulation file to generate a separate INP file for the individual. Then, INP files are submitted in batches for solution calculation.

Step 6. Establishment of fitness function. In GA, the evaluation of a result is not determined by the structure of the solution, but directly by the size of a fitness value. Thus, the objective function must be transformed into a single individual fitness function, which is the only basis to judge the individual optimisation result.[34] Given that there exist two conflicting objectives (the maximum gap elimination rate $f^1(X)$ and the minimum CF value $f^2(X)$) must be satisfied in this optimisation problem, a comprehensive objective function $f(\cdot)$ is proposed, and expressed as $f(\cdot) = (1 - f^1(X)) + f^2(X)$. When the fitness function is minimum, the optimal solution of the algorithm is obtained.

Step 7. Genetic operator operation. In this algorithm, the single point crossover and basic bit mutation strategy is used to complete the crossover and mutation operation, respectively. Roulette algorithm is used to realise the selection operation, the basic idea is that the probability of each individual being selected to the next generation is proportional to its fitness. To accelerate the convergence of algorithm and reduce the fluctuation of optimisation process, multi-point mutation and elite-solution retention strategy are used on the basis of basic genetic operation. This improvement can ensure that the optimal individuals obtained by the previous generation will not be destroyed by crossover and mutation operations to enhance the global search ability of the algorithm.

Step 8. Termination conditions. Given the number limitation of the clamping points and the requirement that no damage occurred in the structure, even in the optimal CF scheme, the clearance elimination rate may not reach 100%. That is, the convergence value of the objective function cannot be predicted. Therefore, here the termination condition is set as a certain amount of computation. Figure 5 explains the implementation of the whole optimisation process for assembly CF layout and magnitude.

Case study

In this section, the proposed multivariable optimisation modelling and calculation method for CF layout and magnitude integrating with improved GA was applied to a real aircraft wing box assembly experiment to validate the feasibility and efficiency. For the considerations of experiment cost and operation convenience, scale-down wing box components are produced. The structure of the wing box comprises two main parts, that is, the skeleton and the panel. The CF optimisation method is applied on the panel assembly. The physical experiment set-up is demonstrated in Figure 6(a). The screw clamping mechanism is used to generate CF and the force value is monitored in real time. The VIC-3D is used to measure the real-time strain, and the shape data of the components are obtained by FARO edge 2.7 shown in Figure 6(b). In this experiment, the panel is made of carbon fibre reinforced epoxy resin matrix composite material. The laminate is divided into 20 layers along the thickness direction, with a nominal thickness of 3.76 mm, and the layup information is $[+45/90/-45/0/90/0/-45/90/+45/-45]$s. The material properties of the composite panel are listed in Table 1. The skeleton is aluminium alloy machining part, and the physical properties of the material are shown in Table 2.

Given the existence of manufacturing defects and the accumulation of assembly errors, especially for composite component, non-compliant assembly inevitably occur. For the assembly process of the wing box

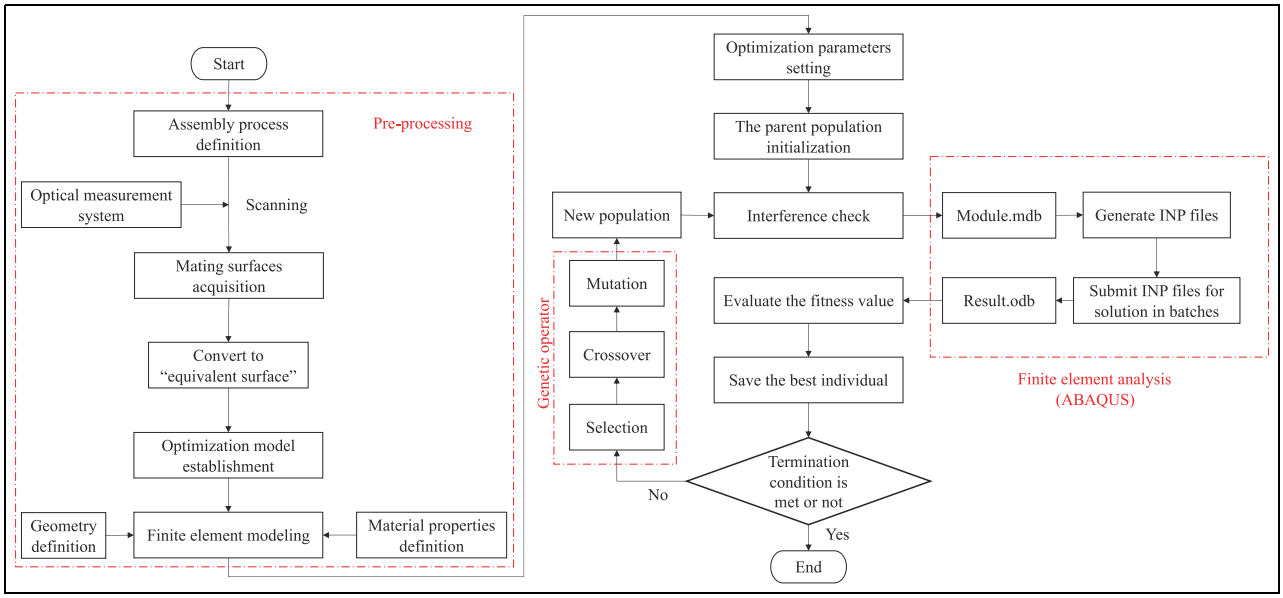

Figure 5. Optimisation procedure for assembly CF layout and magnitude.

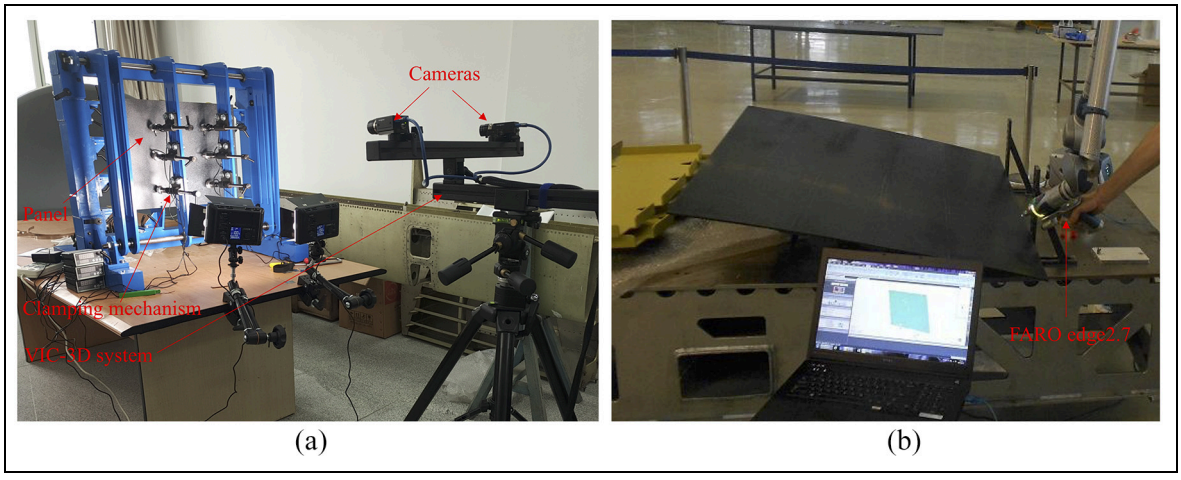

Figure 6. (a) The set-up of physical experiment and (b) the scanning process.

Table 1. Material parameters of the composite panel.

Material properties	Values
Modulus in fibre direction E_1/GPa	156
Transverse moduli $E_2 = E_3$/GPa	8.35
Shear moduli $G_{12} = G_{13}$/GPa	4.32
Shear moduli G_{23}/GPa	2.52
Poisson's ration $\mu_{12} = \mu_{13}$	0.33
Poisson's ration μ_{23}	0.55

Table 2. Material physical properties of the skeleton.

Material properties	Values
Mass density	$2.7 \times 10^3 kg/m^3$
Poisson's ration	0.33
Young's modulus	7.17×10^4MPa

panel and the skeleton in this experiment, the actual mating surfaces are not consistent with the theoretical ones. Therefore, if the form defects and part deformations can be considered when we optimise the assembly CF of the composite panel, then the assembly gap and stress distribution of composite structures can be well controlled and obtain high product performance simultaneously. According to the implementation procedures of the CF layout and magnitude optimisation illustrated in Section 3, the optimal CF scheme can be obtained without damaging the composite structure.

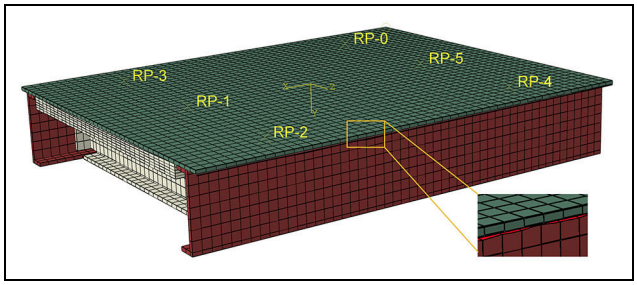

Figure 7. FEA model of the panel and the skeleton.

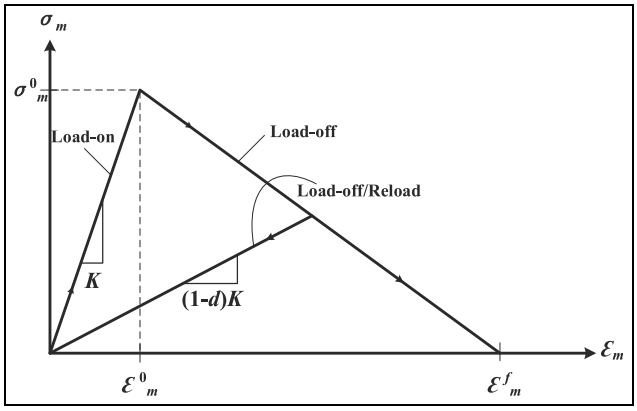

Figure 8. The bilinear constitutive model.

Finite element modelling and model verification

Firstly, the mating surfaces of the real panel and the skeleton are measured and processed. By using the method presented in Section 2, the equivalent skeleton surface is obtained. For the detailed information of point cloud processing, refer to our other article.[4] Thus, the mating surfaces between the actual panel and skeleton can be converted to the matching between the ideal panel surface and the equivalent skeleton surface. Therefore, a parametric FEA model was established on the basis of the theoretical model of the panel and the equivalent skeleton surface, as shown in Figure 7. The dimensional information of the simulation model is consistent with the actual component, including the layer information of the composite laminates.

To evaluate the damage of composite materials, a cohesive unit should be added into the panel. In this study, the traction-separation constitutive model is used to simulate the cohesive unit failure. To effectively predict the response of interface delamination, bilinear constitutive model is adopted.[35,36] The stress–strain curve of bilinear constitutive model shown in Figure 8 presents that when $\varepsilon_m = \varepsilon_m^0$, the material begins to yield, delamination occurs. When $\varepsilon_m = \varepsilon_m^f$, the material completely yields and cracks. Many judgement criteria exist for delamination initiation, and here the secondary stress failure criterion[35] is adopted. The expression is as follows:

$$\left(\frac{\langle \sigma_n \rangle^2}{\sigma_n^0}\right)^2 + \left(\frac{\tau_s}{\tau_s^0}\right)^2 + \left(\frac{\tau_n}{\tau_n^0}\right)^2 = 1 \qquad (5)$$

where, σ_n, τ_s, τ_n represent the contact stress in the normal, first and second shear directions, respectively; $\sigma_n^0, \tau_s^0, \tau_n^0$ represent the maximum contact stress of deformation in the normal, the first and the second shear directions, respectively. The damage evolution criterion is based on the energy release rate, and the Benzeggagh–Kenane failure criterion[37] is used in this FEA model.

Given the gap between the panel and the skeleton, defining the contact relationship and determine the contact properties in the model is necessary. A small slip is used to describe the relative sliding between the contact surfaces, and a friction coefficient 0.1 is set. As to the boundary conditions, because the main research object is the panel, the skeleton surface, which not assembled with the panel is fixed directly, and the symmetrical boundary conditions are applied to the bottom and side of the panel. In the post-processing, to precisely obtain the gap elimination rate, the displacement of all the finite element nodes on the contact area are extracted and calculated.

After the parametric FEA model was established, the model accuracy must be verified. Here a set of comparative experiment was conducted, on the premise that the simulation model parameter setting is consistent with the physical experiment set up. An identical CF scheme was applied on the physical wing box components and the simulation FEA model, respectively. Here, the number of the clamping points was set as six. Taking the centre point of the panel as the origin of the local coordinate system, the positions and the force values of each clamping point are shown in Table 3. Then, 20 points on the panel were chosen randomly as the gap monitoring points. After the pre-set CF scheme was applied on the panel, the gap values were measured by feeler gauges. Also, the distribution of strain field and displacement on the panel surface was recorded by VIC-3D in real-time. VIC-3D is based on the principle of Digital Image Correlation (DIC) and it can accurately measure the displacement and strain of the actual component surface. Accordingly, the same CF scheme is loaded on the FEA model, and the gap value at the same position is recorded as well. Table 4 records the experiment and finite element calculation results obtained at the gap monitoring points. The maximum relative error of the FEA results is not more than the need of general engineering of 0.1 from the experimental data. In addition, the comparison of strain distribution of the panel surface between the FEA model and

Table 3. Positions and force values of clamping points.

	P_1	P_2	P_3	P_4	P_5	P_6
Coordination	(-150, 100)	(-150, 0)	(-150, -150)	(150, -150)	(150, 0)	(150, 150)
Force (N)	110	110	110	110	110	110

Table 4. Comparison of gap value between experiment and finite element results.

Number	Coordination	Gap values (mm)		Relative errors
		Experiment	FEA	
1	(200, 150)	0.35	0.369	0.0543
2	(200, 100)	0.2	0.213	0.065
3	(200, 50)	0.25	0.237	-0.052
4	(200, 0)	0.2	0.183	-0.085
5	(200, -50)	0.1	0.092	-0.08
6	(200, -100)	0.25	0.261	0.044
7	(200, -150)	0.1	0.105	0.05
8	(100, -150)	0.15	0.142	-0.0533
9	(0, -150)	0.3	0.317	0.0567
10	(-100, -150)	0.45	0.463	0.0289
11	(−200, -150)	0.35	0.374	0.0686
12	(-200, -100)	0.2	0.211	0.055
13	(-200, -50)	0.15	0.142	-0.0533
14	(-200, 0)	0.1	0.108	0.08
15	(-200, 50)	0.1	0.103	0.03
16	(-200, 100)	0.2	0.195	-0.025
17	(-200, 150)	0.35	0.329	-0.06
18	(-100, 150)	0.45	0.427	-0.0511
19	(0, 150)	0.3	0.323	0.0767
20	(100, 150)	0.4	0.376	-0.06

the physical experiment is illustrated in Figure 9. The response of the FEA matches the physical experimental data well. The strain in most regions obtained by experiment and the FEA is 0.21 mm and 0.24 mm. Besides, whether in the experiment or the FEA, the position of the maximum strain appears at the place where the CF is applied. Therefore, the aforementioned results show that the established FEA model can be efficiently applied to analyse the stress and deformation of the wing box panel assembly.

Efficiency verification of the CF optimisation algorithm

The efficiency evaluation analyses whether the optimisation algorithm can optimise the distribution and the magnitude of the CF to decrease the assembly stress without damage to the composite structure. The efficiency evaluation has two sections. First, the capability assessment of the CF optimisation process. Second, the assembly force limitation analysis will show whether the composite structure is at the risk of being damaged during the CF adjustment process.

Efficiency analysis of optimisation algorithm

In order to verify the feasibility of the optimisation algorithm, the parametric FEA model demonstrated in previous section was used as an example. The improved GA method was applied to optimise the layout and the magnitude of the CF scheme. Different from random search, GA is a typical iterative algorithm. It can effectively use the information of previous generation to optimise the search pattern and path and infer the better generation through the historical information. The

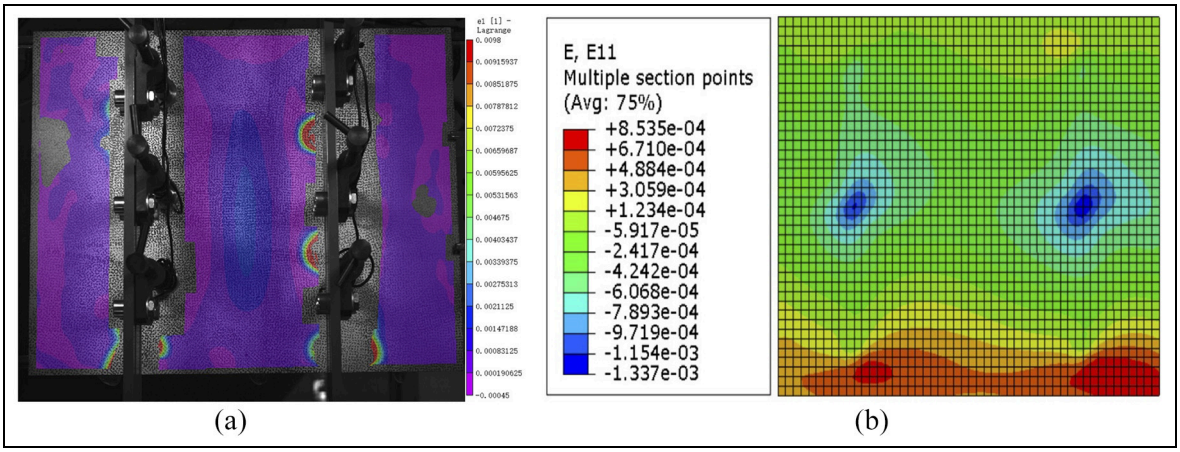

Figure 9. Panel surface strain distribution (a) experiment and (b) FEA simulation.

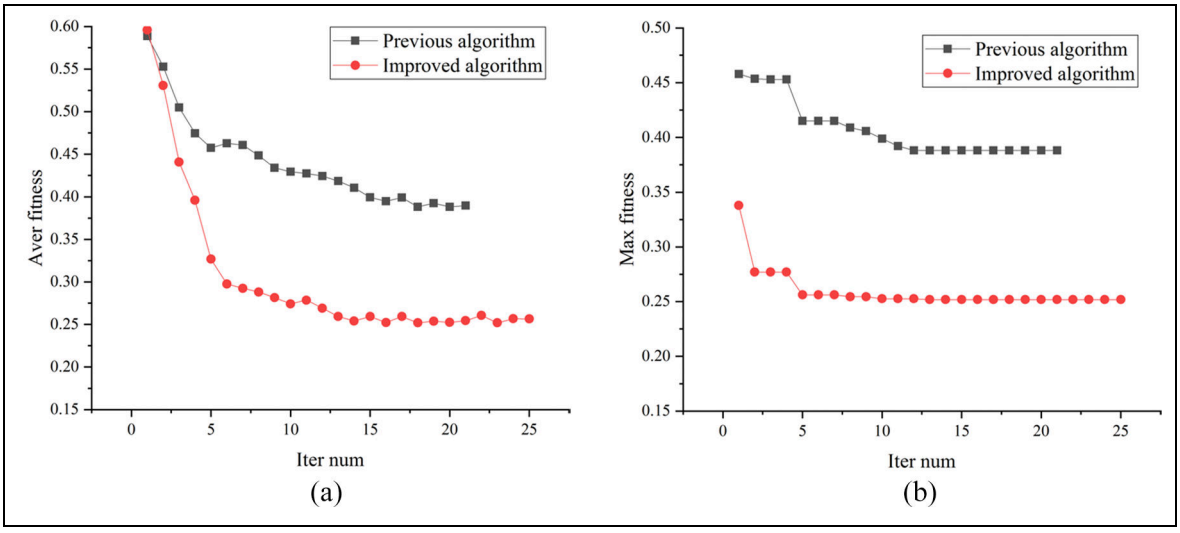

Figure 10. The convergence of fitness function (a) average fitness and (b) maximum fitness.

efficiency and performance of GA are determined by the value of each parameter, including population size N, mutation probability P_m, crossover probability P_c and evolution algebra T.

Population size represents the number of individuals in a population. When the value is small, the calculation speed can be improved to some extent, but the diversity of the population will be sacrificed, which may cause premature phenomenon. However, when the value is large, the computational efficiency and speed decrease greatly. Here we choose $N = 30$. P_m is between (0, 1), which determines whether the offspring individual can participate in the mutation, here we set $P_m = 0.2$. Crossover probability greatly affects the convergence and diversity of the algorithm, and crossover operator is the main method for GA to generate new individuals. Here we set $P_c = 0.6$. The number of iterations T is a parameter representing the termination condition of the algorithm. The optimal individual of the T generation is the optimal solution of the optimisation problem. In this study, the number of iterations $T = 15$, 20, 25 and 35 was tried respectively. Ultimately, it can be found that, increasing the number of iterations can get idea optimisation results and stability of the optimal solution. However, as the number of iterations continues to increase, the objective function is not further optimised but the operational efficiency is reduced. Thus, the iterations T is set as 25. To avoid the algorithm falling into the local optimal solution and accelerate the convergence speed, some improvements are made to the algorithm. Competition selection and multipoint mutation are added into the previous GA. The convergence of fitness function in Figure 10 shows that the improved algorithm can reach the stable solution rapidly. Figure 11 illustrates the layout and magnitude of CF scheme at

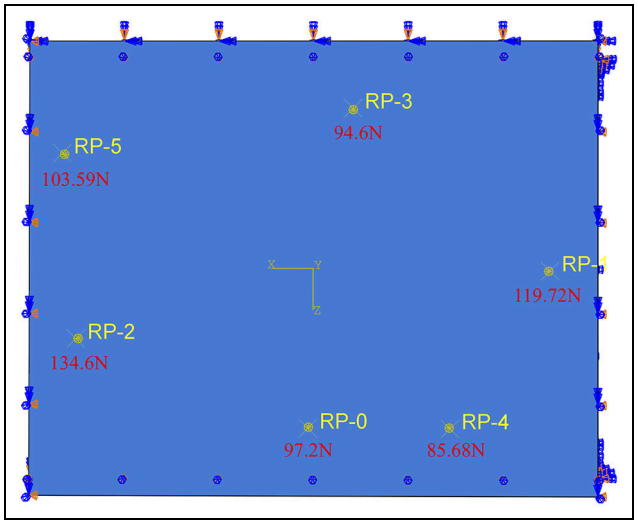

Figure 11. Layout and magnitude of the CF scheme after optimisation.

the optimal state. It can be seen that the optimal CF distribution is consistent with real gap distribution between the two mating surfaces.

To further verify the efficiency of the optimisation model, the commonly used CF layout (300 mm/50 N) for composite part assembly mentioned by Li et al.[11] was set as the contrast group, as shown in Figure 12. After post-processing of the FEA model, we can get the clearance elimination rate and damage indicator. Here 0.2 mm is set as the clearance threshold. According to the statistics of clearance on the finite element nodes, it can be found that the clearance elimination rate of contrast group is 58.29%, and no delamination occurred in the structure. Then the optimal CF layout was applied to the same FEA model,

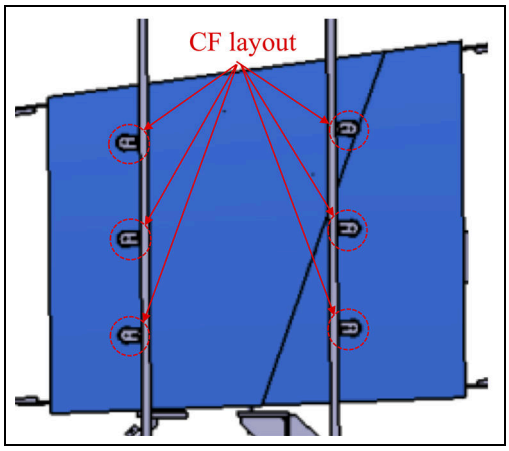

Figure 12. Layout of the CF scheme in other literature.[11]

and the clearance elimination rate reaches 89.32%, which is 53.2% higher than the contrast one. Figure 13(a) displays that relative uniform stresses exist on the panel surface after optimisation, and 70% of the regional stress value is around 25.8 Mpa. Figure 13(b) indicates the displacement distribution on the panel is relatively uniform, and the displacement of most areas along the CF direction is 0.53 mm. Figure 14 represents the SDEG and QUADSCRT values of the cohesive unit. The stress of few elements reached the maximum value, but the SDEG value of all elements is less than 1, hence no delamination damage occurred inside the composite panel. Therefore, by comparing with the commonly used CF layout for composite part assembly, the proposed CF optimisation algorithm for aircraft composite structure assembly can optimise the assembly force layout and magnitude to realise better assembly performance.

Clamping force limitation analysis

In calculating the CF optimisation assembly, the setting of assembly force limit is important because it is related to whether the applied CF will cause damage to the interior of the composite material. Here we analysed the stress response and the SDEG value of the cohesive unit when the assembly forces range from 50 N to 250 N. We adopted the optimal clamping points layout shown in Figure 11 and set all the force value to be identical. We explored the maximum principal stress and equivalent (Von Mises) stress under different magnitudes of assembly forces, as illustrated in Figure 15. In addition, we used the maximum SDEG value as a criterion for judging composite damage. The evolution of composite delamination damage reveals that when

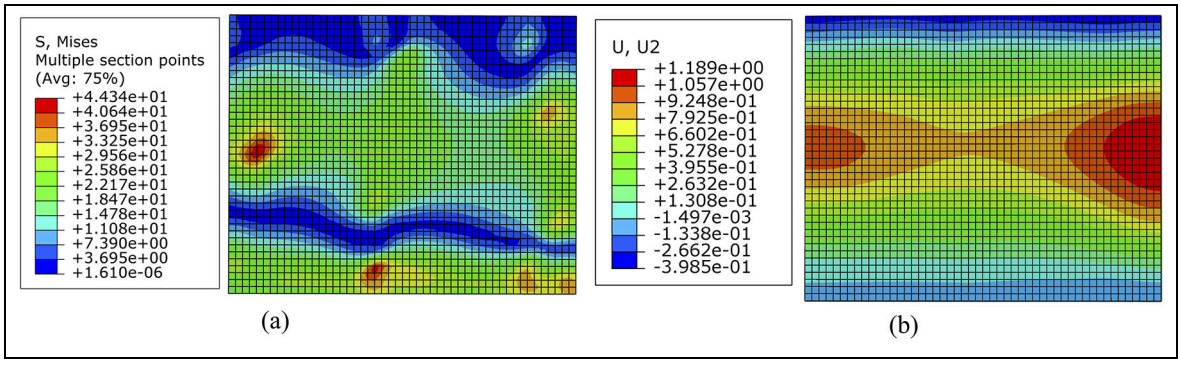

Figure 13. (a) Stress distribution of the panel surface and (b) displacement distribution in U2 direction.

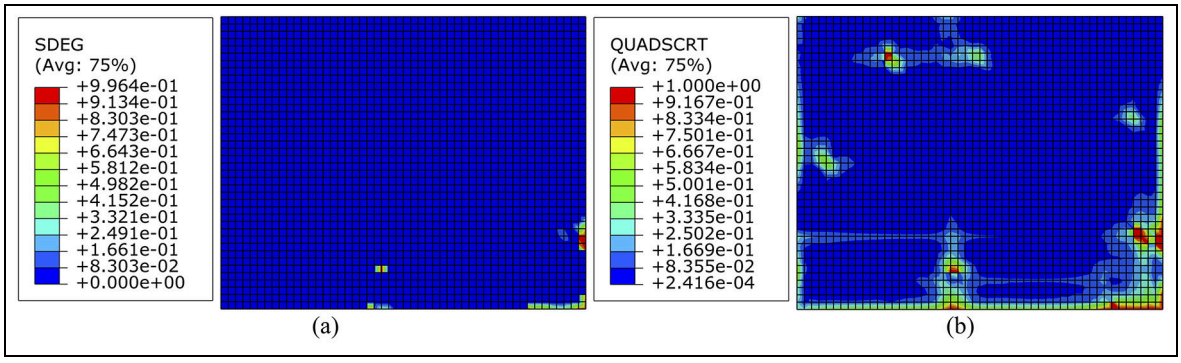

Figure 14. (a) SDEG value and (b) QUADSCRT value of the cohesive unit.

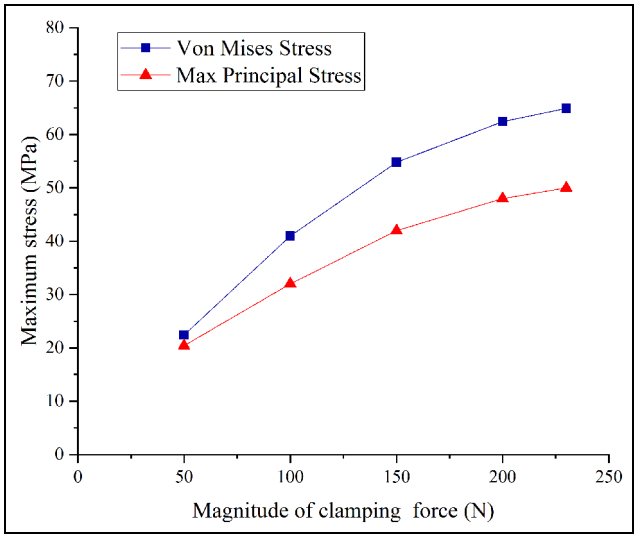

Figure 15. Maximum stress under different magnitudes of clamping force.

the assembly forces are loaded to 230 N, the SDEG value of few elements reached to 1. Thus, for this wing box panel assembly, the permitted CF limitation, which will not damage the composite structure is 230 N. Besides, the maximum principal stress and equivalent (Von Mises) stress at the assembly force limitation is up to 49.8 MPa and 64.9 MPa.

Summary and outlook

Given that manufacturing defects exist in every manufactured part, especially in the composite component, plus the accumulation of assembly errors, the non-compliant assembly are prone to appear between the mating surfaces of the components. In the engineering application, the assembly CF can be used to solve this non-compliant problem, that is, eliminate the assembly gap. An approach for the CF layout and magnitude optimisation is developed in this study, which considered the influence of the form defects and part deformations. In this method, the CF optimisation for composite structure assembly is emphasised and the damage judgement of composite materials is studied. In the pre-processing of the optimisation algorithm, the 'equivalent surface' concept is used to simplify the contact between two non-ideal surfaces. On the basis of the parametric FEA model, a multi-constraint nonlinear optimisation problem is solved by improved GA. Afterward, a real aircraft wing box assembly experiment is conducted to validate the feasibility and efficiency of the proposed method. On the basis of equivalent surface conversion, the established optimisation model can reflect the actual assembly situation accurately. Moreover, the optimal CF scheme can eliminate assembly gaps on the premise of reducing assembly stress. In this study, in view of the non-uniformity of actual assembly clearance, a customised CF scheme is realised, that is, it is adjustable according to the clearance distribution. This method is effective in reducing the assembly gap to enhance the assembly performance. However, this optimal CF layout has high requirements for assembly tooling, more standardised CF scheme considering the assembly tooling structures must be studied in future research works.

Declaration of conflicting interests

The author(s) declared no potential conflicts of interest with respect to the research, authorship and/or publication of this article.

Funding

The author(s) disclosed receipt of the following financial support for the research, authorship and/or publication of this article: This work is supported by the National Natural Science Foundation of China (Grant No. 51975280); National Key Laboratory of Science and Technology on Helicopter Transmission (HTL-O-20G02); China Postdoctoral Science Foundation (2020M671516).

ORCID iDs

Wei Zhang https://orcid.org/0000-0002-8862-9772
Yuan Chen https://orcid.org/0000-0002-9366-3190
Yeping Xiong https://orcid.org/0000-0002-0135-8464

References

1. Kappel E. Spring-in of curved CFRP/foam-core sandwich structures. *Compos Struct* 2015; 128: 155–164.
2. Mezeix L, Seman A, Nasir MNM, et al. Spring-back simulation of unidirectional carbon/epoxy flat laminate composite manufactured through autoclave process. *Compos Struct* 2015; 124: 96–205.
3. Ramirez J and Wollnack J. Flexible automated assembly systems for large CFRP-structures. *Procedia Technol* 2014; 15: 447–455.
4. Zhang W, An L, Sherar P, et al. Posture optimization algorithm for large structure assemblies based on skin model. *Math Probl Eng* 2018; 2018: 12.
5. Zhang Q, An L, Yue X, et al. Optimization of size and layout of pressing force for composite airframe structure assembly based on genetic algorithm. *Acta Mater Compos Sin* 2019; 36: 1546–1557.
6. Maropoulos PG, Muelaner JE, Summers MD, et al. A new paradigm in large-scale assembly—research priorities in measurement assisted assembly. *Int J Adv Manuf Technol* 2014; 70(1–4): 621–633.
7. Jonsson M, Murray T, Robertsson A, et al. Force feedback for assembly of aircraft structures. *SAE technical papers*, 2010.
8. Jonsson M. *On manufacturing technology as an enabler of flexibility: affordable reconfigurable tooling and force-controlled robotics*. Sweden: Linkoäping University, 2013.

9. Wu F, Li D and Du B. Optimal assembly of a skin panel onto the fuselage framework based on force control technology. *Arch Proc Inst Mech Eng Part E J Process Mech Eng* 2015; 230: 1–5.
10. Soäderberg R, Waärmefjord K and Lindkvist L. Variation simulation of stress during assembly of composite parts. *CIRP Ann Manuf Technol* 2015; 64: 17–20.
11. Li DS, Zhai YN and Li XQ. Research and application advances of stress-less assembly methods for composite airframe. *Aeronaut Manuf Technol* 2017; 528: 30–34.
12. Krishnakumar K and Melkote SN. Machining fixture layout optimization using the genetic algorithm. *Int J Mach Tools Manuf* 2000; 40: 579–598.
13. Padmanaban KP, Arulshri KP and Prabhakaran G. Machining fixture layout design using ant colony algorithm based continuous optimization method. *Int J Adv Manuf Technol* 2009; 45: 922–934.
14. Cheng H, Li Y, Zhang K, et al. Optimization method of fixture layout for aeronautical thin-walled structures with automated riveting. *Assem Autom* 2012; 32: 323–332.
15. Lu C and Zhao H. Fixture layout optimization for deformable sheet metal workpiece. *Int J Adv Manuf Technol* 2015; 78: 85–98.
16. Yang B, Wang Z, Yang Y, et al. Optimization of fixture locating layout for sheet metal part by cuckoo search algorithm combined with finite element analysis. *Adv Mech Eng* 2017; 9: 1–10.
17. Chen C, Sun Y and Ni J. Optimization of flexible fixture layout using N-M principle. *Int J Adv Manuf Technol* 2018; 96: 4303–4311.
18. Favreliere H. *Toleä rancement modal, de la meä trologie vers les speä cifications*. PhD Thesis, University of Savoie, 2009.
19. Grandjean J, Ledoux Y and Samper S. On the role of form defects in assemblies subject to local deformations and mechanical loads. *Int J Adv Manuf Technol* 2013; 65: 1769–1778.
20. Yastrebov VA, Anciaux G and Molinari JF. From infinitesimal to full contact between rough surfaces: evolution of the contact area. *Int J Solids Struct* 2015; 52: 83–102.
21. Wang Z, Wang W, Hu Y, et al. A numerical elastic–plastic contact model for rough surfaces. *Tribol Trans* 2010; 53: 224–38.
22. Liu J, Zhang Z, Ding X, et al. Integrating form errors and local surface deformations into tolerance analysis based on skin model shapes and a boundary element method. *Computer Aided Des* 2018; 104: 45–59.
23. Zhao L, Gong Y and Zhang J. A survey on delamination growth behavior in fiber reinforced composite laminates. *Acta Aeronaut et Astronaut Sin* 2019; 40: 522509.
24. Ortiz M and Pandolfi A. Finite-deformation irreversible cohesive elements for three-dimensional crack-propagation analysis. *Int J Numer Meth Eng* 1999; 44(9): 1267–1282.
25. Moes N and Belytschko T. Extended finite element method for cohesive crack growth. *Eng Fract Mech* 2002; 69: 813–833.
26. Turon A, Vila CGD, Camanho PP, et al. An engineering solution for mesh size effects in the simulation of delamination using cohesive zone models. *Eng Fract Mech* 2007; 74: 1665–1682.
27. Turon A, Camanho PP, Costa J, et al. Accurate simulation of delamination growth under mixed-mode loading using cohesive elements: definition of interlaminar strengths and elastic stiffness. *Compos Struct* 2010; 92: 1857–1864.
28. Morris GM, Goodsell DS, Halliday RS, et al. Automated docking using a Lamarckian genetic algorithm and an empirical binding free energy function. *J Comput Chem* 1998; 19: 1639–1662.
29. Costa L and Oliveira PN. An elitist genetic algorithm for multiobjective optimization. *J Baoji College Arts Sci* 2004; 24: 217–236.
30. Fonseca C and Fleming P. An overview of evolutionary algorithms in multiobjective optimization. *Evol Comput* 2014; 3: 1–16.
31. Veldhuizen DAV and Lamont GB. Multiobjective evolutionary algorithms: analyzing the state-of-the-art. *Evol Comput* 2014; 8: 125–147.
32. Che L. Hybrid discrete differential evolution with a self-adaptive penalty function for constrained engineering optimization. *J Mech Eng* 2011; 47: 141.
33. He B, Che L and Liu C. Optimization design of gear based on discrete differential evolution algorithm. *J Mech Transm* 2012; 36: 39–42.
34. Chakraborty B. Genetic algorithm with fuzzy fitness function for feature selection. In: *IEEE international symposium on industrial electronics*, 2002. L'Ayuila, Italy: IEEE Xplore.
35. Camanho PP, Davila CG and De Moura MF. Numerical simulation of mixed-mode progressive delamination in composite materials. *J Compos Mater* 2003; 37: 1415–1438.
36. Reedy ED, Mello FJ and Guess TR. Modeling the initiation and growth of delamination in composite structures. *J Compos Mater* 1997; 31: 812–831.
37. Shokrieh M, Zeinedini A and Ghoreishi SM. On the mixed mode I/I delamination R-curve of E-glass/epoxy laminated composites. *Compos Struct* 2017; 171: 19–31.